

# SCIENTIFIC REPORTS

OPEN

## Cadmium and lithium doping in silver orthophosphate: An *ab initio* study

Yang Huang<sup>1</sup>, Ming-Yang Liu<sup>1</sup>, Tai Ma<sup>1</sup>, Zhong-Ping Lou<sup>1</sup>, Chao Cao<sup>2</sup> & Yao He<sup>1</sup>

Received: 05 February 2016

Accepted: 10 August 2016

Published: 31 August 2016

Using hybrid functional calculations, we investigate the effects of defects and defect complexes related with Cd, Li, and N impurities on the atomic and electronic properties of  $\text{Ag}_3\text{PO}_4$ . It was found that substitutional Cd on Ag lattice site ( $\text{Cd}_{\text{Ag}}$ ) contributes to the *n*-type conductivity of  $\text{Ag}_3\text{PO}_4$ . For substitutional Cd on P (or O) lattice site ( $\text{Cd}_{\text{P}}$ ) (or  $\text{Cd}_{\text{O}}$ ), it is not expected that Cd will incorporate into the P (or O) site due to the strong covalent interactions in the  $\text{PO}_4$  structural units. The interstitial Cd ( $\text{Cd}_i$ ) acts as a shallow donor, but its formation energy is relatively high compared with that of  $\text{Cd}_{\text{Ag}}$ . For the ( $\text{Cd}_{\text{Ag}}-2\text{N}_{\text{O}}$ ) complex, the formation of this inactive complex generates a fully occupied impurity band just above the valence band maximum of  $\text{Ag}_3\text{PO}_4$ , which significantly reduces the acceptor transition energy level. But the formation energy of the ( $\text{Cd}_{\text{Ag}}-2\text{N}_{\text{O}}$ ) complex is even higher than that of the corresponding single point defect  $\text{N}_{\text{O}}$ . Unlike  $\text{Li}_{\text{P}}$  and  $\text{Li}_{\text{O}}$  which has relatively high formation energy, interstitial Li ( $\text{Li}_i$  or  $\text{Li}_i(\text{s})$ ) with an appreciable solubility is likely to be the *n*-type dopant under O-poor condition.

Owing to that fact that oxide semiconductor photocatalysts have promising applications in the development of renewable energy (e.g., converting solar energy into chemical fuels) and the treatment of environment pollution (e.g., degradation of pollutants), much attention has been paid to these materials over the past several decades<sup>1–3</sup>. One of the most popular oxide semiconductors for this purpose, titanium dioxide ( $\text{TiO}_2$ ), based on its high photocatalytic activity, resistance to photocorrosion, low cost and non-toxicity, has received intense research interest as a promising photocatalyst for water splitting and hydrogen production<sup>4,5</sup>. However, the intrinsic wide band gap of pure  $\text{TiO}_2$  (~3.2 eV for anatase and ~3.0 eV for rutile) confines its photon absorption to the ultraviolet (UV) region, severely limiting solar energy utilization to ~5%. Hence great efforts have been made to extend the photoabsorption of  $\text{TiO}_2$  to the visible light region<sup>5–7</sup>. Recently, silver-based oxides semiconductors are reported to own high photocatalytic activation in the visible light region, such as  $\text{Ag}_3\text{VO}_4$ <sup>8</sup>,  $\text{AgGaO}_2$ <sup>9</sup>,  $\text{AgSbO}_3$ <sup>10</sup>. Especially, Ye *et al.*<sup>11</sup> have found that  $\text{Ag}_3\text{PO}_4$  exhibits strong oxidation power leading to  $\text{O}_2$  production from water, and the quantum yield achieve up to nearly 90% under visible light. This is intriguing because most photocatalysts give much poorer quantum yields of ~20%<sup>12</sup>. Therefore, further studies<sup>13–17</sup> were carried out to understand the mechanism of its high water-oxidation activity. For example, Umezawa *et al.*<sup>18</sup> revealed that the excellent photocatalytic performance of  $\text{Ag}_3\text{PO}_4$  is attributed to the Ag *s-s* hybridization without localized *d* states which results in the highly dispersive band structure of the CBM of  $\text{Ag}_3\text{PO}_4$ . Although pure  $\text{Ag}_3\text{PO}_4$  achieves an extremely high quantum yield under visible light, it has been recently found that native point defects are unlikely responsible for the electrical conductivity<sup>12</sup>. However, photoelectrochemical cell needs two-electrode to convert light energy into electric energy, e.g., metal cathode and photoanode made of *n*-type semiconductor<sup>16,19</sup>. Therefore, we expect that external doping can further improve the photocatalytic activity of this novel photooxidation material.

The valence-band maximum (VBM) of  $\text{Ag}_3\text{PO}_4$  composes of mostly Ag *4d* and O *2p* states<sup>20</sup>. Oxygen is much more electronegative than the attempted nitrogen acceptor dopant, and the transition energy level of the  $\text{N}_{\text{O}}$  acceptor should be high. Indeed, the calculated transition level for single acceptor  $\text{N}_{\text{O}}$  is 0.4 eV above the VBM of  $\text{Ag}_3\text{PO}_4$ <sup>17</sup>. On the other hand, since the cohesive energy of  $\text{N}_2$  is large, the chemical potential of  $\text{N}_2$  is very low and the formation energy of  $\text{N}_{\text{O}}$  is very high<sup>21</sup>. To obtain net *p*-type  $\text{Ag}_3\text{PO}_4$ , the low solubility of N monodoping is unlikely to generate sufficient number of holes to compensate the free electrons. Successful *p*-type doping requires a shallow delocalized acceptor level. But doping generally destroys the local symmetry, and the chemical

<sup>1</sup>Department of Physics, Yunnan University, Kunming 650091, China. <sup>2</sup>Department of Physics, Hangzhou Normal University, Hangzhou 310036, China. Correspondence and requests for materials should be addressed to Y.H. (email: yhe@ynu.edu.cn)

mismatch between the host and dopant may result in deep defect levels in the band gap<sup>22</sup>. The codoping method was originally proposed by Yamamoto and Katayama-Yoshida for carrier control in wide-band-gap semiconductors<sup>23</sup>. Using codoping method one may be able to enhance the dopant solubility and lower the defect transition energy levels. However, further study found that although codoping could be useful in increasing dopant incorporation, the different wave function characters and symmetry of donor and acceptor levels may result in a too weak repulsion between these levels, and codoping will fail to reduce the defect transition energy levels<sup>24,25</sup>. In order to decrease the ionization energy of N acceptor in ZnO, Yan *et al.*<sup>25</sup> proposed the impurity band model to explain the real codoping mechanism. The essence of this model is the rise of the VBM. According to the “doping pinning rule”, the lower the VBM of a semiconductor is, the higher the probability that the semiconductor cannot be doped *p*-type is<sup>26</sup>. Moreover, Li *et al.*<sup>27</sup> considered that the anion and cation kinetic *p-d* repulsion was one of the reasons why N<sub>O</sub> defect level is deep in ZnO, if replacing Zn atom by isovalent Mg or Be atom containing no *d* orbital, the defect transition energy level of nX<sub>Zn</sub>-N<sub>O</sub> (X = Mg, Be, n = 1, 2, 3, 4) should be lower than that of N<sub>O</sub> in ZnO. But there is little studies on Li (without occupied *d* orbital) codoping in Ag<sub>3</sub>PO<sub>4</sub>, which will be addressed in this work.

In this present work, we used screened Coulomb potential hybrid DFT calculations to investigate the atomic structure and electronic properties of Cd, Li monodoping and (Cd, N), (Li, N) codoping in Ag<sub>3</sub>PO<sub>4</sub>. We calculate the formation energies and the transition energy levels of Cd<sub>Ag</sub>, Cd<sub>P</sub>, Cd<sub>O</sub>, Cd<sub>i</sub>, Cd<sub>i</sub>(s), the (Cd<sub>Ag</sub>-2N<sub>O</sub>) complex, Li<sub>P</sub>, Li<sub>O</sub>, Li<sub>i</sub>, Li<sub>i</sub>(s), and the (Li<sub>Ag</sub>-N<sub>O</sub>) complex, as well as the binding energies of all defect complexes. The results show that Cd<sub>Ag</sub> and Li<sub>i</sub> (or Li<sub>i</sub>(s)) may serve as possible sources of *n*-type conductivity under O-poor conditions. Cd<sub>Ag</sub> is likely to bind with N<sub>O</sub> to form the (Cd<sub>Ag</sub>-N<sub>O</sub>) complex with a binding energy of -2.02 eV, and doping further N atom results in the (Cd<sub>Ag</sub>-2N<sub>O</sub>) complex, which acts as acceptor with a significantly smaller transition level compared to the isolated N acceptor in Ag<sub>3</sub>PO<sub>4</sub>.

## Methods

Our calculations are based on DFT<sup>28</sup> and projector-augmented wave potentials<sup>29</sup> as implemented in the Vienna *ab initio* simulation package (VASP) code<sup>30</sup>. The exchange correlation potential is treated with the screened hybrid functional of Heyd, Scuseria, and Ernzerhof (HSE)<sup>31</sup>. We find that a proportion of 33% HF exchange with 67% PBE exchange produces accurate values for lattice constants and the band gap in Ag<sub>3</sub>PO<sub>4</sub>. The electron wave function was expanded in plane waves up to a cutoff energy of 300 eV and a Monkhorst-Pack *k*-point mesh<sup>32</sup> of 2 × 2 × 2 was used for geometry optimization and electronic structure calculations. Both the atomic positions and cell parameters were optimized until residual forces were below 0.01 eV/Å. The optimized cell parameters are *a* = *b* = *c* = 6.02 Å, in excellent agreement with the experimental values of *a* = *b* = *c* = 6.00 Å<sup>20</sup>. The calculated indirect band gap (M-Γ) and the direct band gap (Γ) are 2.33 eV and 2.45 eV, in excellent agreement with the experimental value of 2.36 and 2.43 eV, respectively<sup>11</sup>. A 128-atom supercell is used to simulate Cd, Li monodoping and (Cd, N), (Li, N) codoping in Ag<sub>3</sub>PO<sub>4</sub>.

The likelihood of incorporating an impurity in Ag<sub>3</sub>PO<sub>4</sub> is determined by its formation energy. In this paper, the formation energy of a charged defect is defined as the following:<sup>33</sup>

$$\Delta H_f(\alpha, q) = \Delta E(\alpha, q) + \sum n_i \mu_i + qE_F \quad (1)$$

$$\text{where, } \Delta E(\alpha, q) = E(\alpha, q) - E(\text{host}) + \sum n_i E(i) + q\varepsilon_{\text{VBM}}(\text{host}) \quad (2)$$

A more detailed discussion of the formation energy is described elsewhere<sup>34,35</sup>. When Ag<sub>3</sub>PO<sub>4</sub> is grown under thermal equilibrium conditions, the chemical potentials of the constituent atoms, which is referenced to the values of their elemental forms, must satisfy the equilibrium condition  $3\mu_{\text{Ag}} + \mu_{\text{P}} + 4\mu_{\text{O}} = \Delta H_f(\text{Ag}_3\text{PO}_4) = -10.46$  eV, where  $\Delta H_f(\text{Ag}_3\text{PO}_4)$  is the formation enthalpy of Ag<sub>3</sub>PO<sub>4</sub>. In addition, we must enforce the constraint such as  $2\mu_{\text{Ag}} + \mu_{\text{O}} < \Delta H_f(\text{Ag}_2\text{O})$ , to prevent the precipitation of Ag<sub>2</sub>O during the growing process of Ag<sub>3</sub>PO<sub>4</sub>. Similar constraint must be applied to P<sub>2</sub>O<sub>5</sub><sup>17</sup>. To avoid the precipitation of constituent atoms,  $\mu_{\text{Ag}}, \mu_{\text{P}}, \mu_{\text{O}}$  must satisfy  $\mu_{\text{Ag}} < 0, \mu_{\text{P}} < 0, \mu_{\text{O}} < 0$ , respectively. For impurity doping, the chemical potentials of impurities also need to satisfy other constraints to avoid the formation of impurities-related phases. Specifically, the chemical potential of Cd is constrained by  $\mu_{\text{Cd}} < 0$  and  $\mu_{\text{Cd}} + \mu_{\text{O}} < \Delta H_f(\text{CdO}) = -2.59$  eV (experimental value<sup>36</sup>: -2.68 eV and theoretical value<sup>36</sup>: -2.40 eV). Also for Li doping, the chemical potential of Li is constrained by  $\mu_{\text{Li}} < 0$  and  $2\mu_{\text{Li}} + \mu_{\text{O}} < \Delta H_f(\text{Li}_2\text{O}) = -5.96$  eV (experimental value<sup>37</sup>: -6.20 eV and theoretical value<sup>38</sup>: -6.28 eV). We take  $\mu_{\text{N}}$  with respect to the energy per atom of N<sub>2</sub> molecule.

The binding energy of a complex defect represents energy changing from isolated dopants to a complex defect. To determine whether the binding of two dopants is energetically preferred (e.g., Cd<sub>Ag</sub> and N<sub>O</sub>), we calculate the binding energy  $E_b$ , which is defined as<sup>39-41</sup>

$$E_b = \Delta H_f(\text{Cd}_{\text{Ag}}, q_1) + \Delta H_f(\text{N}_{\text{O}}, q_2) - \Delta H_f(\text{Cd}_{\text{Ag}}-\text{N}_{\text{O}}, q_3) \quad (3)$$

where  $q_1, q_2$ , and  $q_3$  are the most stable charge states of Cd<sub>Ag</sub>, N<sub>O</sub>, and complex (Cd<sub>Ag</sub>-N<sub>O</sub>), respectively, at any given  $E_F$ . A positive  $E_b$  indicates the reaction is exothermic and the defect pair tends to bind to each other when both are present in the system.

## Results and Discussion

**Cd monodoping.** Cadmium sits to the right of Ag in the periodic table, having an atomic size very close to that of Ag which makes sure that negligible strain energy is introduced to the Ag<sub>3</sub>PO<sub>4</sub> host. Thus, we expect Cd to preferentially occupy the Ag site in Ag<sub>3</sub>PO<sub>4</sub>, leading to relatively small relaxations and acting as a shallow donor. Indeed, in the neutral charge state (Cd<sub>Ag</sub><sup>0</sup>), the neighboring O atoms relax inward, resulting in a Cd-O

Cd							
Donor	$\varepsilon(0/+)$	$\varepsilon(0/2+)$	$\varepsilon(0/3+)$	$\varepsilon(0/4+)$	$E_b$	$\Delta H_f$ (O-rich)	$\Delta H_f$ (O-poor)
Cd <sub>Ag</sub>	0.01					0.43	-0.42
Cd <sub>O</sub>	-0.02	-0.24	0.53	0.91		8.59	5.21
Cd <sub>i</sub>	0.27	0.14				4.74	3.05
Cd <sub>i</sub> (s)	0.1	0.01				4.90	3.21
Acceptor	$\varepsilon(-/0)$	$\varepsilon(2-/0)$	$\varepsilon(3-/0)$	$\varepsilon(4-/0)$	$E_b$	$\Delta H_f$ (O-rich)	$\Delta H_f$ (O-poor)
Cd <sub>p</sub>	0.13	0.27	0.25			7.89	10.42
Cd <sub>Ag</sub> -2N <sub>O</sub>	0.49				0.51	8.80	4.57
Cd <sub>Ag</sub> -2V <sub>Ag</sub>	0.18				-0.08		
N <sub>O</sub>	0.46					5.46	3.77
V <sub>Ag</sub>	0.18					0.46	1.35
Li							
Donor	$\varepsilon(0/+)$	$\varepsilon(0/2+)$	$\varepsilon(0/3+)$	$\varepsilon(0/4+)$	$E_b$	$\Delta H_f$ (O-rich)	$\Delta H_f$ (O-poor)
Li <sub>O</sub>	0.18	1.55	2.0			5.90	3.37
Li <sub>i</sub>	-0.04					2.22	1.38
Li <sub>i</sub> (s)	-0.15					2.16	1.32
Acceptor	$\varepsilon(-/0)$	$\varepsilon(2-/0)$	$\varepsilon(3-/0)$	$\varepsilon(4-/0)$	$E_b$	$\Delta H_f$ (O-rich)	$\Delta H_f$ (O-poor)
Li <sub>p</sub>	0.70	0.69	0.85	0.89		6.62	10.0
Li <sub>Ag</sub> -N <sub>O</sub>	0.54				-0.11	3.51	1.82
Li <sub>Ag</sub> -V <sub>Ag</sub>	-0.04				0.04		

**Table 1.** Calculated transition energy levels and binding energies  $E_b$  of the defect complexes, and defect formation energies with  $E_F = 0$  under O-rich and O-poor conditions in Ag<sub>3</sub>PO<sub>4</sub>. All energies are in eV.

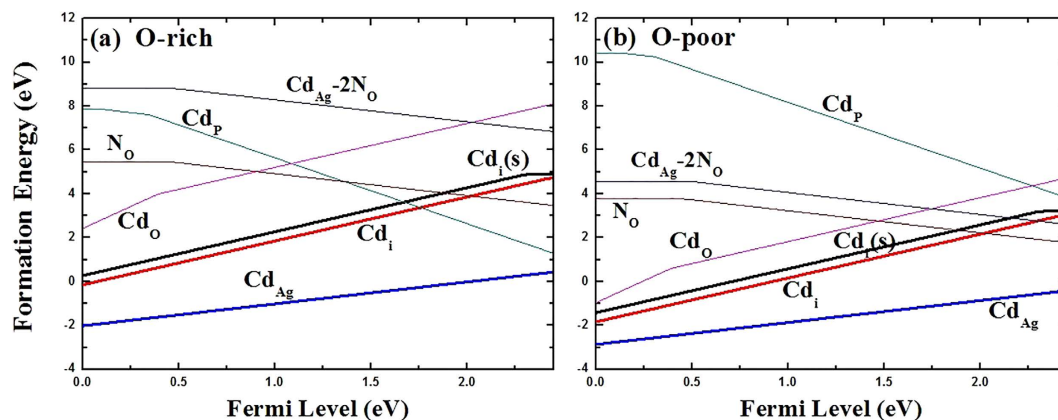


**Figure 1.** The formation energies of possible Cd monodoped defects, Cd<sub>Ag</sub>, Cd<sub>p</sub>, Cd<sub>O</sub>, Cd<sub>i</sub> and Cd<sub>i</sub>(s), together with (Cd<sub>Ag</sub>-2N<sub>O</sub>) complex as a function of the Fermi energy under O-rich (a) and O-poor (b) conditions. Only the lowest formation energy states are shown.

bond length (2.21 Å) that is 6.8% shorter than the equilibrium Ag-O bond length (2.37 Å), while the Cd-Ag bond length (3.22 Å) becomes 7% longer than the equilibrium Ag-Ag bond length (3.01 Å). In the positive charge state (Cd<sub>Ag</sub><sup>+</sup>), the Cd-O bond length is 2.2 Å, and the Cd-Ag bond length is 3.23 Å. It is noteworthy that the Cd-O bond length is similar to the counterpart (2.35 Å) in CdO unit cell<sup>42</sup>.

As expected, Cd<sub>Ag</sub> is shallow donor, and the transition energy level of  $\varepsilon(0/+)$  is located at 0.01 eV below the CBM. The conductivity of a semiconductor depends not only on the transition levels of donor or acceptors, but also on their formation energies. The results of formation energy for the defects under consideration are listed in Table 1. Figure 1 shows the calculated formation energies of Cd<sub>Ag</sub> as a function of Fermi level under O-rich [Fig. 1(a)] and O-poor [Fig. 1(b)] conditions, respectively. Under O-poor growth condition [Fig. 1(b)], the formation energy of Cd<sub>Ag</sub> is much lower than that under O-rich condition, and becomes negative in the entire range of  $E_F$  value in the band gap. This is because the chemical potential of Cd is limited by the O chemical potential due to the limit of impurity-related phase CdO. Therefore, the highest possible  $\mu_{Cd}$  requires the lowest  $\mu_O$ , i.e. O-poor condition. Our results suggest that *n*-type Ag<sub>3</sub>PO<sub>4</sub> is achievable by Cd-doping under O-poor condition.

When Cd dopant occupies the P lattice site, this defect behaves as a triple acceptor. The transition energy levels of  $\varepsilon(-/0)$ ,  $\varepsilon(2-/0)$  and  $\varepsilon(3-/0)$  are located at 0.13 eV, 0.27 eV and 0.25 eV above the VBM, respectively. In general, deep impurity-related levels typically represent localized electron distributions, and a change of occupancy usually results in change of structures<sup>43</sup>. Indeed, because of the large size mismatch between the Cd and P atoms,

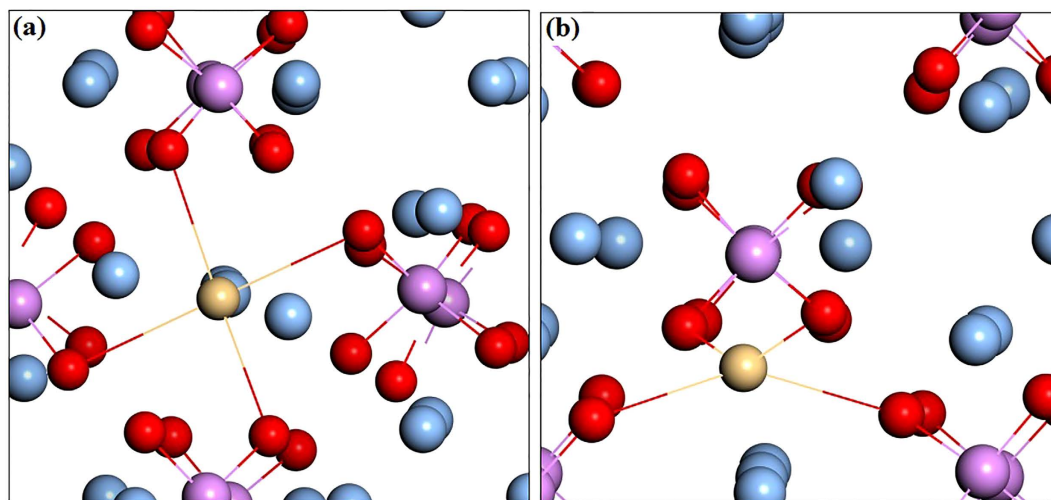


**Figure 2.** Atomic geometry of the relaxed structures of the (a)  $Cd_i$  and (b)  $Cd_i(s)$  configurations in  $Ag_3PO_4$ .

the four oxygen neighbors of  $Cd_p$  lie at a distance of 2.20–2.21 Å, which are larger than the equilibrium P–O bond length of 1.56 Å for bulk  $Ag_3PO_4$ . As seen in Fig. 1, the formation energy of  $Cd_p$  is quite high even under extreme O-rich condition. Moreover, recent studies, based on a revised molecular orbital diagram for  $Ag_3PO_4$ , have pointed out that the strong covalent interactions are formed in the tetrahedral  $PO_4$  structural units<sup>14</sup>. It is therefore not expected that Cd will incorporate on the P site with an appreciable solubility.

Since oxygen atom can provide six electrons and cadmium can provide only two electrons, it is expected that  $Cd_o$  acts as donor. Indeed, the calculated transition energy levels of  $\varepsilon(0/+)$ ,  $\varepsilon(0/2+)$ ,  $\varepsilon(0/3+)$  and  $\varepsilon(0/4+)$  are located at  $-0.02$  eV,  $-0.24$  eV,  $0.53$  eV and  $0.91$  eV below the CBM, respectively. For  $Cd_o$ , in the 0, 1+, 2+, 3+ and 4+ charge states, the distances between Cd and the nearest-neighbor O atoms are 3.32, 3.05, 2.88, 2.86 and 2.84 Å, respectively. This dramatic lattice distortion can lead to higher formation energy. According to Fig. 1,  $Cd_o$  has much lower formation energy under O-poor condition than under O-rich condition. But even under O-poor condition,  $Cd_o$  has a formation energy that is 1.91 eV higher than that of  $Cd_{Ag}$  at the VBM, and so its contribution is less significant.

For interstitial Cd, we have studied two possible atomic configurations. One is the tetrahedral site coordinated by four O atoms (expressed as  $Cd_i$ ), the other is the so-called split interstitial site which consists of two atoms on a single substitutional lattice site (expressed as  $Cd_i(s)$ ), as shown in Fig. 2. For  $Cd_i(s)$ , this configuration is 0.16 eV higher in energy than  $Cd_i$ , and the calculated transition energy levels of  $\varepsilon(0/+)$  and  $\varepsilon(0/2+)$  are located at 0.27 eV and 0.14 eV below the CBM, which are 0.17 eV and 0.13 eV higher than that of  $Cd_i$ , respectively. Therefore, in the following discussion we consider only the  $Cd_i$  configuration. In the neutral charge state, the distance between Cd and the nearest-neighbor O atom is 2.33 Å which is very close to the Cd–O bond length in CdO unit cell. In the 1+ and 2+ charge states, the Cd–O bond lengths are 2.29 and 2.26 Å, respectively. As shown in Fig. 1, the calculated formation energies of  $Cd_i^{2+}$  are  $-0.14$  and  $-1.83$  eV under O-rich and O-poor conditions at the VBM, respectively. It implies that O-poor condition would produce much more abundant numbers of Cd donors in comparison with O-rich condition. However, its formation energy is relatively high compared with that of  $Cd_{Ag}$  under both O-rich and O-poor conditions, regardless of the Fermi level position. Our results indicate that  $Cd_i$  will not be a relevant configuration for Cadmium in  $Ag_3PO_4$ .

**Cd codoping.** The formation of the  $(Cd_{Ag}-N_o)$  complex is a result of Coulomb binding between positively charged donor ( $Cd_{Ag}$ ) and negatively charged acceptor ( $N_o$ ). To see if the complex can form, we calculated the binding energy. We find that  $Cd_{Ag}$  is likely to bind with  $N_o$  to form the  $(Cd_{Ag}-N_o)$  complex with a binding energy of 0.03 eV. The positive binding energy means that the complex is energetically favorable and can be seen as the passive complex. Obviously, the  $(Cd_{Ag}-N_o)$  complex is dielectric and will not provide electron or hole in  $Ag_3PO_4$ . But it may affect the electrical properties by changing the electronic structure<sup>44</sup>. The values of  $E_b$  for this complex are shown in Fig. 3 as a function of the Fermi level. Figure 4 shows the calculated total DOS of  $Ag_3PO_4$  with and without the  $(Cd_{Ag}-N_o)$  complex in order to see the effect of passivation on relative shift of the VBM. As can be seen from Fig. 4, the formation of a passive  $(Cd_{Ag}-N_o)$  complex does not change the basic electronic structure, but only generates an additional fully occupied impurity band with the energy width of 0.54 eV above the VBM of  $Ag_3PO_4$ . The distance between Cd and N in the complex is 2.14 Å. The bond length of Cd and its nearest-neighbor O atom is 2.18 Å, which is 8% shorter than the equilibrium Ag–O bond length. The Cd–Ag bond length (3.01 Å) becomes 2% longer than the equilibrium Ag–Ag bond length.

When a second N atom is added to a neighbor site of the passive  $(Cd_{Ag}-N_o)$  complex (the configuration of  $Cd_{Ag}-2N_o$  complex is shown in Fig. 5), we find that the binding energy of  $(Cd_{Ag}-2N_o)$  is 0.51 eV with respect to the  $(Cd_{Ag}-N_o)$  complex and  $N_o$ . The positive binding energy means that the *p*-type complex is energetically stable and can form if more acceptors are doped into  $Ag_3PO_4$ . Based on the fact that the transition will occur between the N defect levels and the fully occupied impurity bands rather than the original valence band<sup>25</sup>, we calculated the transition energy level  $\varepsilon(-/0)$  of  $(Cd_{Ag}-2N_o)$  which is 0.49 eV above the VBM of  $Ag_3PO_4$ . And the value is

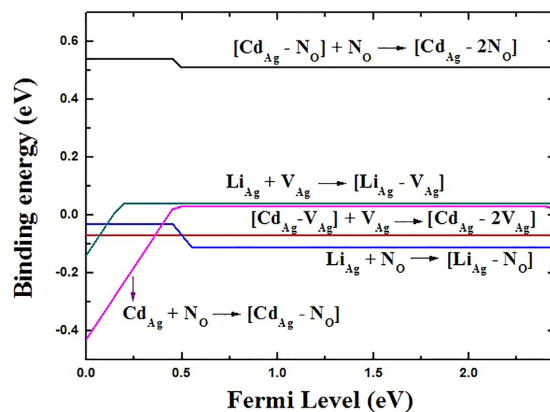


Figure 3. Binding energies  $E_b$  of complex defects as a function of the Fermi level.

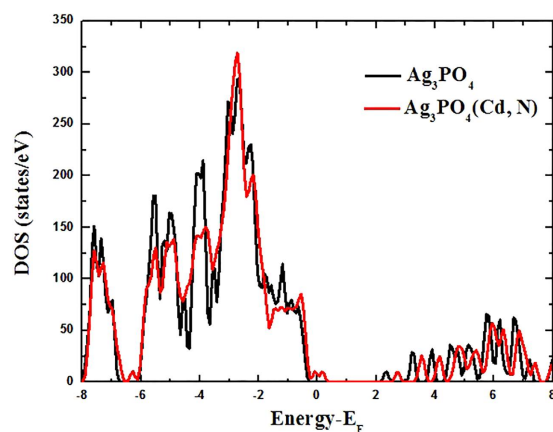


Figure 4. The calculated total DOS for pure  $\text{Ag}_3\text{PO}_4$  and a supercell containing a  $(\text{Cd}_{\text{Ag}}-\text{N}_{\text{O}})$  complex.

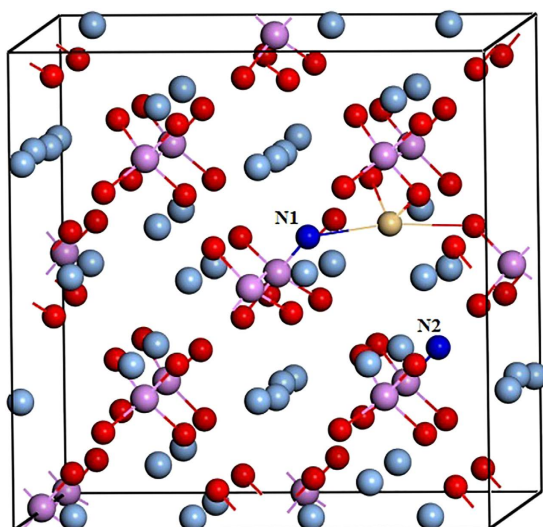
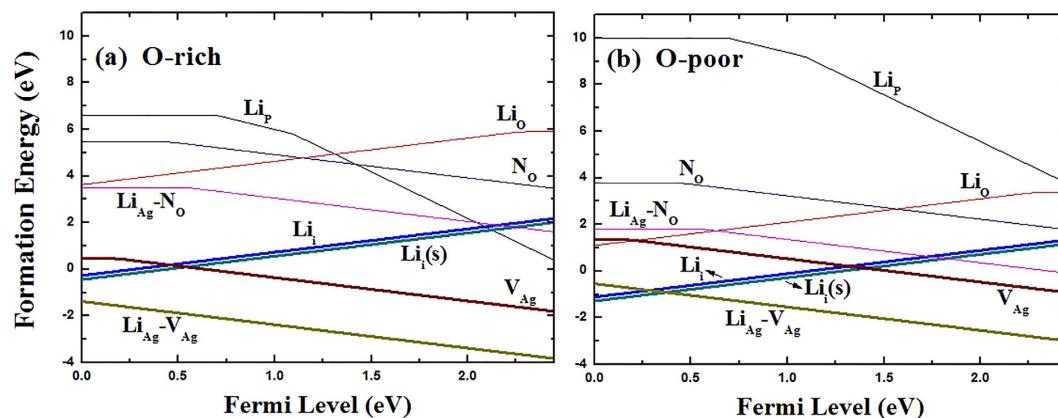


Figure 5. Crystal structure of  $\text{Ag}_3\text{PO}_4$  supercell with codoping of  $\text{Cd}_{\text{Ag}}$  and two  $\text{N}_{\text{O}}$ . The silver, pink, red, khaki and blue balls represent Ag, P, O, Cd and N atoms, respectively.

reduced to  $-0.05$  eV from the impurity band of the passive  $(\text{Cd}_{\text{Ag}}-\text{N}_{\text{O}})$  complex. Therefore, the transition level can be reduced dramatically. In the neutral charge state  $(\text{Cd}_{\text{Ag}}-2\text{N}_{\text{O}})^0$ , the distances between Cd and N1, Cd and N2 atoms in the complex are 2.16 and 4.09 Å, respectively. The bond lengths of Cd-O and N1-P are 2.18 and 1.65 Å,



**Figure 6.** The formation energies of possible Li monodoped defects,  $\text{Li}_p$ ,  $\text{Li}_o$ ,  $\text{Li}_i$  and  $\text{Li}_i(s)$ , together with  $(\text{Li}_{\text{Ag}}-\text{N}_o)$  complex and  $(\text{Li}_{\text{Ag}}-\text{V}_{\text{Ag}})$  complex as a function of the Fermi energy under O-rich (a) and O-poor (b) conditions. Only the lowest formation energy states are shown.

which are 8% shorter and 5.8% longer than the Ag-O and O-P bond lengths in the bulk, respectively. The distance between Cd and Ag is 3.12 Å along the b axis, which is 3.7% longer than the corresponding bond length of Ag-Ag in bulk  $\text{Ag}_3\text{PO}_4$ . Whether a dopant can be a good acceptor, it should have high solubility under proper conditions, except low transition energy. Figure 1 has depicted the calculated formation energies as a function of Fermi level for  $(\text{Cd}_{\text{Ag}}-2\text{N}_o)$  under O-rich and O-poor conditions, respectively. We can see that the formation energy of the  $(\text{Cd}_{\text{Ag}}-2\text{N}_o)$  acceptor is relatively high even under O-poor condition. If the formation energy is higher than that of the corresponding single point defects  $\text{Cd}_{\text{Ag}}$  and  $\text{N}_o$ <sup>17</sup>, it is because the energy cost to create the extra single point defect is larger than the Coulomb interaction between the donors and acceptors<sup>24</sup>. Thus, *p*-type conductivity would not be readily achieved by (Cd, N) codoping of  $\text{Ag}_3\text{PO}_4$ .

From what has been discussed above,  $\text{Cd}_{\text{Ag}}$  is suggested to be the dominant donor in Cd-doped  $\text{Ag}_3\text{PO}_4$ . Combined with the fact that “electron killer” is  $\text{Ag}$  vacancy ( $\text{V}_{\text{Ag}}$ )<sup>16</sup>, the natural candidate for a possible complex is the  $\text{Cd}_{\text{Ag}}$  donor and  $\text{V}_{\text{Ag}}$  acceptor pair. Indeed, our hybrid functional calculations indicate that the  $(\text{Cd}_{\text{Ag}}-2\text{V}_{\text{Ag}})$  complex is an acceptor with the transition level  $\varepsilon(-/0)$  of 0.18 eV above the VBM. In order to increase the distance between two  $\text{V}_{\text{Ag}}$  and weaken the level repulsion between them, we have established a configuration that two  $\text{V}_{\text{Ag}}$  acceptors are connected by  $\text{Cd}_{\text{Ag}}$  donor, as proposed by Limpijumnong *et al.*<sup>45</sup> in  $\text{ZnO}$  ( $\text{As}_{\text{Zn}}-2\text{V}_{\text{Zn}}$ ). However, the binding energy for the  $(\text{Cd}_{\text{Ag}}-2\text{V}_{\text{Ag}})$  complex is negative at  $-0.08$  eV. It implies that this kind of defect complex is unlikely to exist in  $\text{Ag}_3\text{PO}_4$ .

**Li monodoping.** Since Li and Ag are isovalent, Ag substituted by Li ( $\text{Li}_{\text{Ag}}$ ) is electrically inactive and Li monodoping is not considered. Similar to  $\text{Cd}_p$ ,  $\text{Li}_p$  has rather high formation energies under both O-rich and O-poor conditions (as shown in Fig. 6) because of the strong covalent interaction in the  $\text{PO}_4$  units, which indicates that the formation of  $\text{Li}_p$  is energetically unfavorable. The calculated results are summarized in Table 1. In the neutral charge state, the four equivalent oxygen atoms move outward by 25% of the initial P-O bond length. For Li substituting O ( $\text{Li}_o$ ), the calculated formation energies of  $\text{Li}_o$  are lower than  $\text{Li}_p$ , mainly because of the small misfit of atomic radius. The distance between Li and the nearest-neighbor O atom is 1.9 Å in the neutral charge state, and this highly perturbed structure can be described as Li going to an interstitial site and leaving behind an O vacancy<sup>43</sup>. The calculated transition energy levels  $\varepsilon(0/+)$ ,  $\varepsilon(0/2+)$  and  $\varepsilon(0/3+)$  are located at 0.18 eV, 1.55 eV and 2.0 eV below the CBM, respectively.

Although substitutional Li behaves as an acceptor, Li tends to occupy the interstitial site and lose its outmost electron to behave as a donor. This will lead to the self-compensation and limit its application as an efficient *p*-type dopant in  $\text{ZnO}$ <sup>27</sup>. Therefore, we have also studied two possible atomic configurations for interstitial Li as shown in Fig. 7. The most stable configuration is the split interstitial doping and  $\text{Li}_i(s)$  is only 0.06 eV lower in energy than  $\text{Li}_i$ . The calculated transition energy level  $\varepsilon(0/+)$  for  $\text{Li}_i$  and  $\text{Li}_i(s)$  are found to lie at 0.04 and 0.15 eV above the CBM, respectively. Figure 6 shows the calculated defect formation energy as a function of the Fermi level under O-rich and O-poor conditions. From Fig. 6, it was found that Li impurity prefers interstitial sites over substitutional sites regardless of the Fermi level position. For example, the formation energy of  $\text{Li}_i$  ( $\text{Li}_i(s)$ ) is 2.21 eV (2.38 eV) lower than that of  $\text{Li}_o$  under O-poor condition. However, the formation energies of the positively charged interstitial Li ( $\text{Li}_i$  or  $\text{Li}_i(s)$ ) increase with the Fermi energy while the negatively charged complex ( $\text{Li}_{\text{Ag}}-\text{V}_{\text{Ag}}$ ) decrease with the Fermi energy and the  $(\text{Li}_{\text{Ag}}-\text{V}_{\text{Ag}})$  complex is not stable (see discussion later). Our analysis suggests that interstitial Li ( $\text{Li}_i$  or  $\text{Li}_i(s)$ ) is likely to be the *n*-type dopant under O-poor condition.

**Li codoping.** Because  $\text{Li}_{\text{Ag}}$  is electrically inactive and  $\text{N}_o$  is a deep acceptor, the  $(\text{Li}_{\text{Ag}}-\text{N}_o)$  complex is an acceptor. The calculated transition energy level  $\varepsilon(-/0)$  for the complex is located at 0.54 eV above the VBM, deeper than the corresponding single N dopant (0.46 eV)<sup>17</sup>. It is because the radius of Li is very different from Ag. To make sure whether the complex can form, we have also calculated the binding energy. The calculated binding energy for the  $(\text{Li}_{\text{Ag}}-\text{N}_o)$  complex is negative ( $-0.11$  eV), indicating that  $\text{Li}_{\text{Ag}}$  will not bind with  $\text{N}_o$  in  $\text{Ag}_3\text{PO}_4$ .

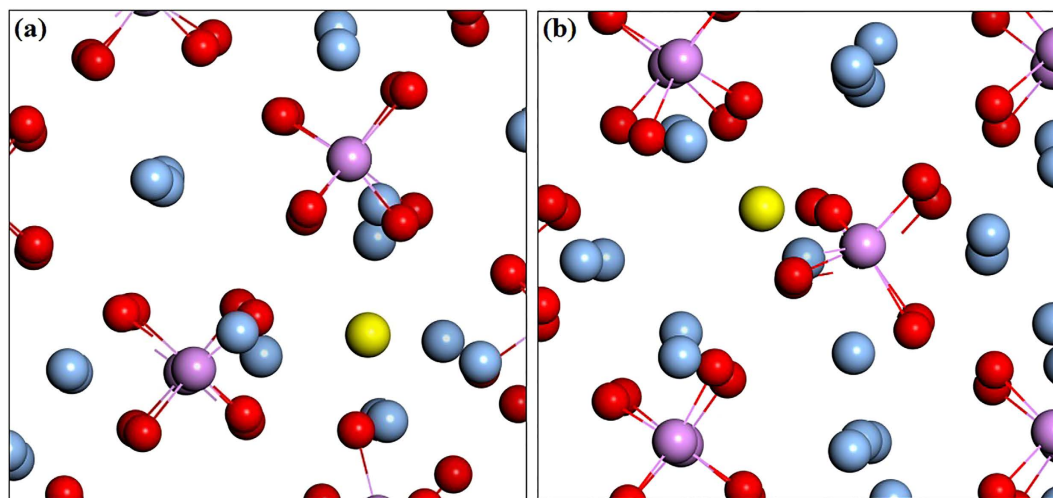


**Figure 7.** Atomic geometry of the relaxed structures of the (a)  $\text{Li}_i$  and (b)  $\text{Li}_i(\text{s})$  configurations in  $\text{Ag}_3\text{PO}_4$ .

This is likely because the Ag-N bond is stronger than the Li-N bond. According to our calculations, the Ag-N bond length (2.11 Å) is shorter than the Li-N bond length (4.61 Å). It should be that the stable  $p$ -type conductivity will not be achieved by the  $(\text{Li}_{\text{Ag}}-\text{N}_{\text{O}})$  complex. We also calculated the transition energy level  $\varepsilon(-/0)$  for the  $(\text{Li}_{\text{Ag}}-\text{V}_{\text{Ag}})$  complex, which is located at 0.04 eV below the VBM. The binding energy of this complex is positive (0.04 eV), which implies that this complex is stable in  $\text{Ag}_3\text{PO}_4$ .

## Conclusions

In summary, we have investigated the formation of isolated defects and defect complexes in Cd and Li monodoped, (Cd, N) and (Li, N) codoped  $\text{Ag}_3\text{PO}_4$  by the hybrid functional calculations. It is found that  $\text{Cd}_{\text{Ag}}$  contributes to the  $n$ -type conductivity of  $\text{Ag}_3\text{PO}_4$  under O-poor conditions. For  $\text{Cd}_{\text{p}}$  and  $\text{Cd}_{\text{O}}$ , both of the two configurations will not be the relevant configurations for Cd doping in  $\text{Ag}_3\text{PO}_4$ , on account of the strong covalent interactions in the tetrahedral  $\text{PO}_4$  structural units. For interstitial Cd ( $\text{Cd}_i$ ), the calculated formation energy is relatively high compared with that of  $\text{Cd}_{\text{Ag}}$  donor. Our results demonstrate that Cd can bind to N atom to form a stable passive  $(\text{Cd}_{\text{Ag}}-\text{N}_{\text{O}})$  complex. Although the transition energy level of the acceptor  $(\text{Cd}_{\text{Ag}}-2\text{N}_{\text{O}})$  complex is reduced from 0.49 to  $-0.05$  eV when electrons are transitioned from the impurity band of the passive complex rather than the original valence band, the formation energy of the acceptor complex is high in comparison with the isolated  $\text{N}_{\text{O}}$ . Same as  $\text{Cd}_{\text{p}}$  and  $\text{Cd}_{\text{O}}$ ,  $\text{Li}_{\text{p}}$  and  $\text{Li}_{\text{O}}$  will not be the relevant configurations for Li doping in  $\text{Ag}_3\text{PO}_4$ . But interstitial Li ( $\text{Li}_i$  or  $\text{Li}_i(\text{s})$ ) with suitable level and appreciable solubility is likely to be the  $n$ -type dopant under O-poor condition. For the  $(\text{Li}_{\text{Ag}}-\text{N}_{\text{O}})$  complex, the calculated binding energy is negative ( $-0.11$  eV) because the Ag-N bond is stronger than the Li-N bond. While, the  $(\text{Li}_{\text{Ag}}-\text{V}_{\text{Ag}})$  complex is potentially to be the  $p$ -type dopant under O-rich condition.

## References

- Hoffman, M. R., Martin, S. T., Choi, W. T. & Bahnemann, D. W. Environmental Applications of Semiconductor Photocatalysis. *Chem. Rev.* **95**, 69 (1995).
- Wang, J., Meng, Q., Huang, J., Li, Q. & Yang, J. L. Band structure engineering of anatase  $\text{TiO}_2$  by metal-assisted P-O coupling. *J. Chem. Phys.* **140**, 174705 (2014).
- Li, P., Umezawa, N., Abe, H. & Ye, J. Novel visible-light sensitive vanadate photocatalysts for water oxidation: implications from density functional theory calculations. *J. Mater. Chem. A* **3**, 10720 (2015).
- Fujishima, A. & Honda, K. Electrochemical Photolysis of Water at a Semiconductor Electrode. *Nature* **238**, 37 (1972).
- Run, L. & Niall, J. E. Band gap engineering of (N, Si)-codoped  $\text{TiO}_2$  from hybrid density functional theory calculations. *New J. Phys.* **14**, 053007 (2012).
- Gai, Y., Li, J., Li, S.-S., Xia, J.-B. & Wei, S.-H. Design of Narrow-Gap  $\text{TiO}_2$ : A Passivated Codoping Approach for Enhanced Photoelectrochemical Activity. *Phys. Rev. Lett.* **102**, 036402 (2009).
- Yin, W.-J., Wei, S.-H., Al-Jassim, M. M. & Yan, Y. Double-Hole-Mediated Coupling of Dopants and Its Impact on Band Gap Engineering in  $\text{TiO}_2$ . *Phys. Rev. Lett.* **106**, 066801 (2011).
- Konta, R., Kato, H., Kobayashi, H. & Kudo, A. Photophysical properties and photocatalytic activities under visible light irradiation of silver vanadates. *Phys. Chem. Chem. Phys.* **5**, 3061 (2003).
- Maruyama, Y., Irie, H. & Hashimoto, K. Visible Light Sensitive Photocatalyst, Delafossite Structured  $-\alpha\text{AgGaO}_2$ . *J. Phys. Chem. B* **110**, 23274 (2006).
- Kako, T., Kikugawa, N. & Ye, J. Photocatalytic activities of  $\text{AgSbO}_3$  under visible light irradiation. *Catal. Today* **131**, 197 (2008).
- Yi, Z. *et al.* An orthophosphate semiconductor with photooxidation properties under visible light irradiation. *Nat. Mater.* **9**, 559 (2010).
- Reunchan, P. & Umezawa, N. Native defects and hydrogen impurities in  $\text{Ag}_3\text{PO}_4$ . *Phys. Rev. B* **87**, 245205 (2013).
- Botelho, G., Sczancoski, J. C., Andres, J., Gracia, L. & Longo, E. Experimental and Theoretical Study on the Structure, Optical Properties, and Growth of Metallic Silver Nanostructures in  $\text{Ag}_3\text{PO}_4$ . *J. Phys. Chem. C* **119**, 6293 (2015).
- Kahk, J. M. *et al.* The electronic structure of silver orthophosphate: experiment and theory. *J. Mater. Chem. A* **2**, 6092 (2014).
- Ma, X. G. *et al.* Origin of Photocatalytic Activation of Silver Orthophosphate from First-principles. *J. Phys. Chem. C* **115**, 4680 (2011).
- Reunchan, P. & Umezawa, N. Sulfur and Silicon Doping in  $\text{Ag}_3\text{PO}_4$ . *J. Phys. Chem. C* **119**, 2284 (2015).

17. Huang, Y., Ma, T., Chen, Q. Y., Cao C. & He, Y. The electronic properties of impurities (N, C, F, Cl, and S) in  $\text{Ag}_3\text{PO}_4$ : A hybrid functional method study. *Sci. Rep.* **5**, 12750 (2015).
18. Umezawa, N., Ouyang, S. & Ye, J. Theoretical study of high photocatalytic performance of  $\text{Ag}_3\text{PO}_4$ . *Phys. Rev. B* **83**, 035202 (2011).
19. Tryk, D. A., Fujishima, A. & Honda, K. Recent topics in photoelectrochemistry: achievements and future prospects. *Electrochimica Acta* **45**, 2363 (2000).
20. Liu, J. J., Fu, X. L., Chen, S. F. & Zhu, Y. F. Electronic structure and optical properties of  $\text{Ag}_3\text{PO}_4$  photocatalyst calculated by hybrid density functional method. *Appl. Phys. Lett.* **99**, 191903 (2011).
21. Duan, X. Y., Yao, R. H. & Zhao, Y. J. The mechanism of Li, N dual-acceptor co-doped p-type ZnO. *Appl. Phys. A* **91**, 467 (2008).
22. Huda, M. N., Yan, Y. & Al-Jassim, M. M. The delocalized nature of holes in (Ga, N) cluster-doped ZnO. *J. Phys.: Condens. Mater* **24**, 415503 (2012).
23. Yamamoto, T. & Katayama-Yoshida, H. Materials Design for the Fabrication of Low-Resistivity p Type GaN Using a Codoped Method. *Jpn. J. Appl. Phys.* **36**, L180 (1997).
24. Wei, S.-H. & Zhang, S. B. Chemical trends of defect formation and doping limit in II-VI semiconductors: The case of CdTe. *Phys. Rev. B* **66**, 155211 (2002).
25. Yan, Y., Li, J., Wei, S.-H. & Al-Jassim, M. M. Possible Approach to Overcome the Doping Asymmetry in Wideband Gap Semiconductors. *Phys. Rev. Lett.* **98**, 135506 (2007).
26. Zhang, S. B., Wei, S.-H. & Zunger, A. A phenomenological model for systematization and prediction of doping limits in II-VI and I-III-VI compounds. *J. Appl. Phys.* **83**, 3192 (1998).
27. Li, J., Wei, S.-H., Li, S.-S. & Xia, J.-B. Design of shallow acceptors in ZnO: First-principles band structure calculations. *Phys. Rev. B* **74**, 081201(R) (2006).
28. Kohn, W. & Sham, L. J. Self-Consistent Equations Including Exchange and Correlation Effects. *Phys. Rev.* **140**, A1133 (1965).
29. Blöchl, P. E. Projector augmented-wave method. *Phys. Rev. B* **50**, 17953 (1994).
30. Kresse, G. & Joubert, D. From ultrasoft pseudopotentials to the projector augmented-wave method. *Phys. Rev. B* **59**, 1758 (1999).
31. Heyd, J., Scuseria, G. E. & Ernzerhof, M. Hybrid functionals based on a screened Coulomb potential. *J. Chem. Phys.* **118**, 8207 (2003).
32. Monkhorst, H. J. & Pack, J. D. Special points for Brillouin-zone integrations. *Phys. Rev. B* **13**, 5188 (1976).
33. Wei, S.-H. Overcoming the doping bottleneck in semiconductors. *Comput. Mater. Sci.* **30**, 337 (2004).
34. Freysoldt, C. *et al.* First-principles calculations for point defects in solids. *Rev. Mod. Phys.* **86**, 253 (2014).
35. Zhang, S. B., Wei, S.-H., Zunger, A. & Katayama-Yoshida, H. Defect physics of the  $\text{CuInSe}_2$  chalcopyrite semiconductor. *Phys. Rev. B* **57**, 9642 (1998).
36. Pandey, M. & Jacobsen, K. W. Heats of formation of solids with error estimation: The mBEEF functional with and without fitted reference energies. *Phys. Rev. B* **91**, 235201 (2015).
37. Lide, David R. ed. *CRC Handbook of Chemistry and Physics, 90th Edition (Internet Version 2010)*, CRC Press/Taylor and Francis, Boca Raton, FL. (2010).
38. Xu, H. Stability of intrinsic defects and defect clusters in  $\text{LiNbO}_3$  from density functional theory calculations. *Phys. Rev. B* **78**, 174103 (2008).
39. Duan, X. M., Stampfl, C., Bilek, M. M. M. & McKenzie, D. R. Codoping of aluminum and gallium with nitrogen in ZnO: A comparative first-principles investigation. *Phys. Rev. B* **79**, 235208 (2009).
40. Raebiger, H., Nakayama, H. & Fujita, T. Control of defect binding and magnetic interaction energies in dilute magnetic semiconductors by charge state manipulation. *J. Appl. Phys.* **115**, 012008 (2014).
41. Raebiger, H., Lany, S. & Zunger, A. Impurity Clustering and Ferromagnetic Interactions that are not Carrier Induced in Dilute Magnetic Semiconductors: The Case of  $\text{Cu}_2\text{O}:\text{Co}$ . *Phys. Rev. Lett.* **99**, 167203 (2007).
42. Burbano, M., Scanlon, D. O. & Watson, G. W. Sources of conductivity and doping limits in CdO from hybrid density functional theory. *J. Am. Chem. Soc.* **133**, 15065 (2011).
43. Wardle, M. G., Goss, J. P. & Briddon, P. R. Theory of Li in ZnO: A limitation for Li-based p-type doping. *Phys. Rev. B* **71**, 155205 (2005).
44. Li, W. *et al.* Investigation on the Formation Mechanism of In-In Codoped p-Type ZnCdO Thin Films: Experiment and Theory. *J. Phys. Chem. C* **118**, 22799 (2014).
45. Limpjumnong, S., Zhang, S. B., Wei, S.-H. & Park, C. H. Doping by Large-Size-Mismatched Impurities: The Microscopic Origin of Arsenic-or Antimony-Doped p-type Zinc Oxide. *Phys. Rev. Lett.* **92**, 155504 (2004).

## Acknowledgements

This work was supported by National Natural Science Foundation of China (Grant No. 61366007 and No. 11164032 and No. 61066005), Program for New Century Excellent Talents in University (Grant No. NCET-12-1080), Applied Basic Research Foundation of Yunnan Province (Grant No. 2011CI003 and No. 2013FB007), Program of high-end scientific and technological talents in Yunnan Province (Grant No. 2013HA019), Program for Excellent Young Talents in Yunnan University, the Scholarship Award for Excellent Doctoral Student granted by Yunnan Province. Computational resources were provided by the High Performance Computing Center of Yunnan University.

## Author Contributions

Y.H. carried out the DFT calculations and prepared the manuscript. M.Y.L., T.M., Z.P.L., C.C. and Y.H. contributed the discussion and suggestions. All authors read the manuscript.

## Additional Information

**Competing financial interests:** The authors declare no competing financial interests.

**How to cite this article:** Huang, Y. *et al.* Cadmium and lithium doping in silver orthophosphate: An *ab initio* study. *Sci. Rep.* **6**, 32574; doi: 10.1038/srep32574 (2016).



This work is licensed under a Creative Commons Attribution 4.0 International License. The images or other third party material in this article are included in the article's Creative Commons license, unless indicated otherwise in the credit line; if the material is not included under the Creative Commons license, users will need to obtain permission from the license holder to reproduce the material. To view a copy of this license, visit <http://creativecommons.org/licenses/by/4.0/>

© The Author(s) 2016